Check for updates

Investigating the exotic magnetic properties in manganese diboride, a borophene intercalation compound

Hui Li[1,2], Siwen Cui[1], Yi Huang[2], Yongsheng Zhao[3]*, Pinwen Zhu[1] and Shuailing Ma[4]*

[1]State Key Laboratory of Superhard Materials, College of Physics, Jilin University, Changchun, China, [2]College of Mathematics and Physics, Guangxi Minzu University, Nanning, China, [3]Deutsches Elektronen-Synchrotron DESY, Hamburg, Germany, [4]Institute of High-Pressure Physics School of Physical Scientific and Technology, Ningbo University, Ningbo, China

The temperature-dependent magnetic susceptibility combined with first-principle calculations was conducted to unravel the magnetic structure and the magnetic interaction of the laminar structure of manganese diboride (MnB_2). MnB_2 showed weak ferromagnetic, antiferromagnetic, and paramagnetic behavior with increased temperature. Its weak ferromagnetic property below 135.6 K Curie temperature (T_C) originated from the spin canting antiferromagnetic magnetic structure. The exotic kink of temperature-dependent magnetic susceptibility at 330 K Néel temperature (T_N) correlated with the transition from antiferromagnetic to paramagnetic structure. First-principle calculation show that the antiferromagnetic ordering show lower energy, and suggest a canting anti-ferromagnetic ordering for its ferromagnetic behavior. The peculiar magnetic behavior of MnB_2 may be due to the insertion of the honeycomb boron layers into the host matrix of manganese atoms. The honeycomb boron layers played a key role in the exchange between two manganese layers. This study resolved the longstanding puzzle of the magnetic structure of MnB_2 and provided a typical laminar magnetic structure prototype.

1 Introduction

Manganese compounds continue to be the hotpot of intensive studies that discovered numerous novel and appealing physical properties, including Mott insulation (e.g., MnO), Peierls distortion (e.g., MnB_4), and super-paramagnetism (e.g., Mn_3O_4) [1–3]. A manganese atom is an extraordinary magnetic prototype of the atoms of transition metals (TMs). According to Hund's rule, manganese atoms have the largest magnetic moment among the 3d TMs. Manganese exhibits weak antiferromagnetic properties since its atoms have close atomic distances between them [4]. Traditionally, inserting other elements into the host matrix of the manganese crystal structure or placing manganese atoms in other crystal frameworks will expand the distance between manganese atoms. Moreover, doping foreign elements or inserting foreign frameworks can tailor the magnetic properties of manganese atoms. Manganese compounds exhibit different magnetic phenomena according to the

different expanded atomic distances between manganese atoms, such as super-paramagnetism (e.g., Mn_3O_4), colossal magnetoresistance (e.g., $La_{0.67}Ca_{0.33}MnO_3$), ferromagnetic (e.g., MnB), spin glass (e.g., CuMn) [5–7].

Transition metal borides are important hard or superhard functional materials due to the rich magnetic behaviors, high hardness, high melting point and excellent thermal stability [8,9]. Manganese diboride (MnB_2) with an AlB_2-type structure is an extraordinary borophene intercalation compound (BIC). Foreign atoms or molecules are inserted between the two-dimensional honeycomb sheets of borophenes to form BICs, leading to ordered structures [10]. Since electrons are accepted or donated between borophenes and metal intercalants, this structure usually modifies the electronic configuration compared with the parent materials, and the final product has a more superior behavior. BIC structures have a rare magnetic behavior, making them ideal systems for probing magnetic interactions. The magnetic behavior of MnB_2 with AlB_2-type structure has been subject to debate for a long time, ever since it was synthesized in the experiment [11]. Andersson et al. and Cadeville reported that MnB_2 exhibited weak ferromagnetic behavior under 143 and 157 K Curie temperature (T_C) with about 0.2 μ_B/Mn magnetic moment [12,13]. However, the magnetic structure derived using the nuclear magnetic resonance (NMR) experiment results was antiferromagnetic with about 3 μ_B/Mn magnetic moment [14,15]. Neutron diffraction can effectively determine magnetic structure. However, Legrand and Neov proposed that the magnetic moment was perpendicular to the c plane with a magnetic moment of 2.6 μ_B/Mn from the neutron diffraction profile due to the inability of neutron diffraction to detect the magnetic structure of borides [15]. Meanwhile, the magnetic structure and magnetic moment they proposed could not explain the experimentally weak ferromagnetic behavior below T_C. Although a theoretical calculation based on Kübler's covalent magnetism was consistent with the magnetic moment deduced from neutron diffraction, the metallic electrical conductivity characteristics contradicted this covalent scenario [16]. None of the earlier experimental results captured this important phenomenon. Consequently, investigating the magnetic structure in this exotic laminar structure is urgent.

This study examined the magnetic properties of MnB_2 experimentally and theoretically to investigate the magnetic structure and magnetic interactions between manganese atoms to hopefully reconcile the incompatible explanations. Some exotic magnetic behaviors were detected in the temperature-dependent magnetic susceptibility. A spin-canting antiferromagnetic magnetic structure was proposed to explain the exotic behaviors detected in the experiments.

2 Experiment and calculation details

Polycrystalline specimens of MnB_2 were prepared using the high pressure and high temperature (HPHT) method described in Ref. [17]. The authors of this study used Rietveld refinements to determine the crystal structure in a previous study. The magnetic susceptibility of the polycrystalline specimen of MnB_2 was measured using a magnetic property measurement system (MPMS, Quantum Design MPMS 3) with a magnetic field of 500 Oe in the 4–400 K temperature range. First, the specimen was cooled down to 5 K without a magnetic field, i.e., zero-field cooled (ZFC). Subsequently,

FIGURE 1
Powder X-ray diffraction pattern and schematic view of the crystal structure of MnB_2.
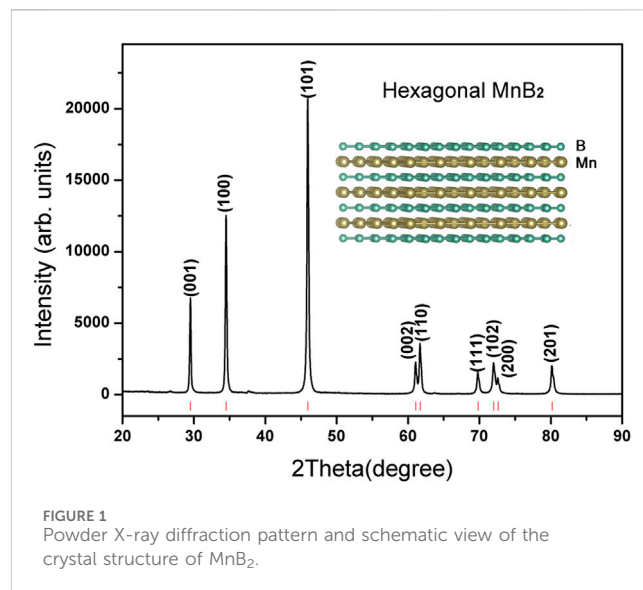
the magnetic field of 500 Oe was applied, followed by heating to 400 K and cooling to 5 K, i.e., field cooled (FC). The hysteresis loop for MnB_2 was measured at different temperatures at 5, 100, 200, and 300 K in the magnetic field ranging from −5,000 Oe to 5,000 Oe.

The stability of structure is the premise of calculating and studying various properties of materials [18,19]. And the structural stability of MnB_2 with AlB_2-type structure has revealed by first-principles calculations and experiments [20,21]. In this context, the Vienna Ab initio Simulation Package (VASP) code with pseudo-potentials plane-wave method was adopted to perform first principle calculations to obtain the equilibrium geometry and ground energy of different magnetic configurations [22]. To determine the magnetic ordering of MnB_2, the energies of MnB_2 with ferromagnetic order and antiferromagnetic order were calculated. The exchange-correlation function was considered through the Perdew–Burk–Ernzerhof (PBE) exchange-correlation function in the generalized gradient approximation (GGA) [23]. Convergence studies showed that the plane-wave cutoff of 500 eV and a dense Monkhorst–Pack grid with a reciprocal space resolution of $2\pi \times 0.03$ Å^{-1} ensured that the total energies converged better than 1 meV/atom [22,24].

3 Results and discussions

MnB_2 was prepared using the HPHT method described in an earlier study [17]. The X-ray diffraction pattern is displayed in Figure 1 with space group P6/mmm, and it can be presented by alternating graphene-like layers made of either B or Mn atoms along the c-axis. The lattice interstices of hexagonal close-packed (hcp) TMs are filled to form AlB_2-type transition metal borides (TMBs). Generally, inserting boron frameworks into the host matrix of pure transition metals (TMs) expands the distance between the atoms of TMs. For example, the lattice parameters of TiB_2 increased by 2.47% and 8.90% along the a- and c-axes compared with titanium, respectively [25]. In manganese metal, the distance between the neighboring atoms manganese atoms is 2.7679 and 2.8041 Å. The distances between the nearest manganese atoms in MnB_2 are 3.007 and 3.037. It is shown that the honeycomb boron layer is
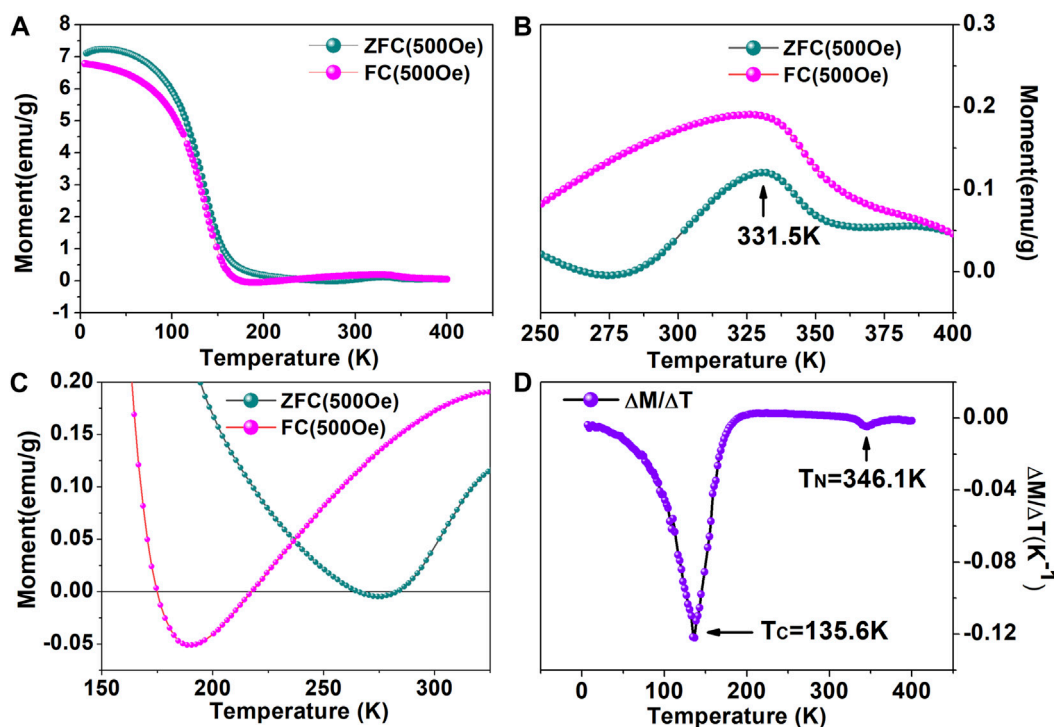
FIGURE 2
(A) Temperature dependence of ZFC and FC magnetizations in an applied field of 500 Oe for MnB$_2$. **(B,C)** The partial enlarged view of Figure **(A,D)** The derivative of magnetization with temperature.

inserted into the main matrix of the manganese lattice and the distance between the manganese atoms is enlarged.

The successful synthesis of high-quality polycrystalline MnB$_2$ allows the probing of its intrinsic magnetic properties. It is well known that manganese, a 3d TM, with nearly half-filled 3d shells, often prefers antiferromagnetic spin ordering. But according to the theory proposed by E. Legrand, the 3 Å distance between manganese atoms would give rise to a complex magnetic structure and magnetic behavior due to the complex exchange interaction [17]. The magnetic behaviors of the polycrystalline MnB$_2$ specimen were investigated using MPMS. As shown in Figures 2A–C, the temperature-dependent magnetization susceptibility curve of MnB$_2$ was measured in the temperature range of 5–400 K in an applied magnetic field of 500 Oe. The most striking thing was that the ZFC curve was higher than the FC curve, contradicting the behavior of traditional magnetic materials. In Figure 2D, T$_C$, defined as the temperature at which $\partial M/\partial T$ is a minimum, was about 135.6 K for the polycrystalline MnB$_2$ specimen. Notably, the weak ferromagnetic ordering was destroyed due to the thermal vibration at 135.6 K since the magnetic coupling was extremely weak in this laminar structure. The kink at 346.1 K could be assigned as the Néel temperature (T$_N$) due to the transition from antiferromagnetic to paramagnetic.

The hysteresis loops of MnB$_2$ measured at the temperatures of 5, 100, 200, and 300 K are shown in Figure 3. At relatively low temperatures of 5 and 100 K, the hysteresis loops exhibited typical ferromagnetic behaviors with saturation magnetization and coercive field. As the temperature exceeded 200 K, the ferromagnetic property was suppressed, and the magnetic
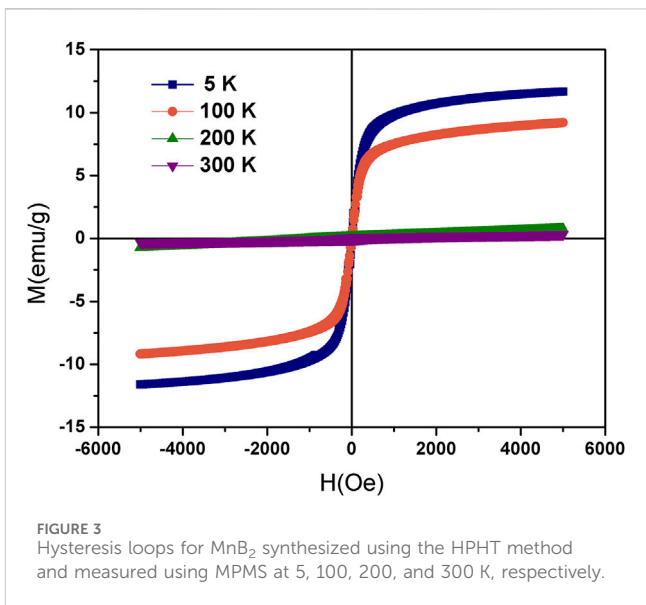

FIGURE 3
Hysteresis loops for MnB$_2$ synthesized using the HPHT method and measured using MPMS at 5, 100, 200, and 300 K, respectively.

hysteresis loop was a straight line with a typical paramagnetic behavior. Khmelevskyi and Mohn proposed that the weak ferromagnetism measured in earlier experiments could be ascribed to the possible secondary magnetic phase in the specimen [16]. In manganese borides, only FeB-type MnB exhibited ferromagnetic properties [26,27]. The X-ray diffraction pattern showed that the synthesized specimen had high purity with no secondary phase diffraction peaks. So, weak ferromagnetic
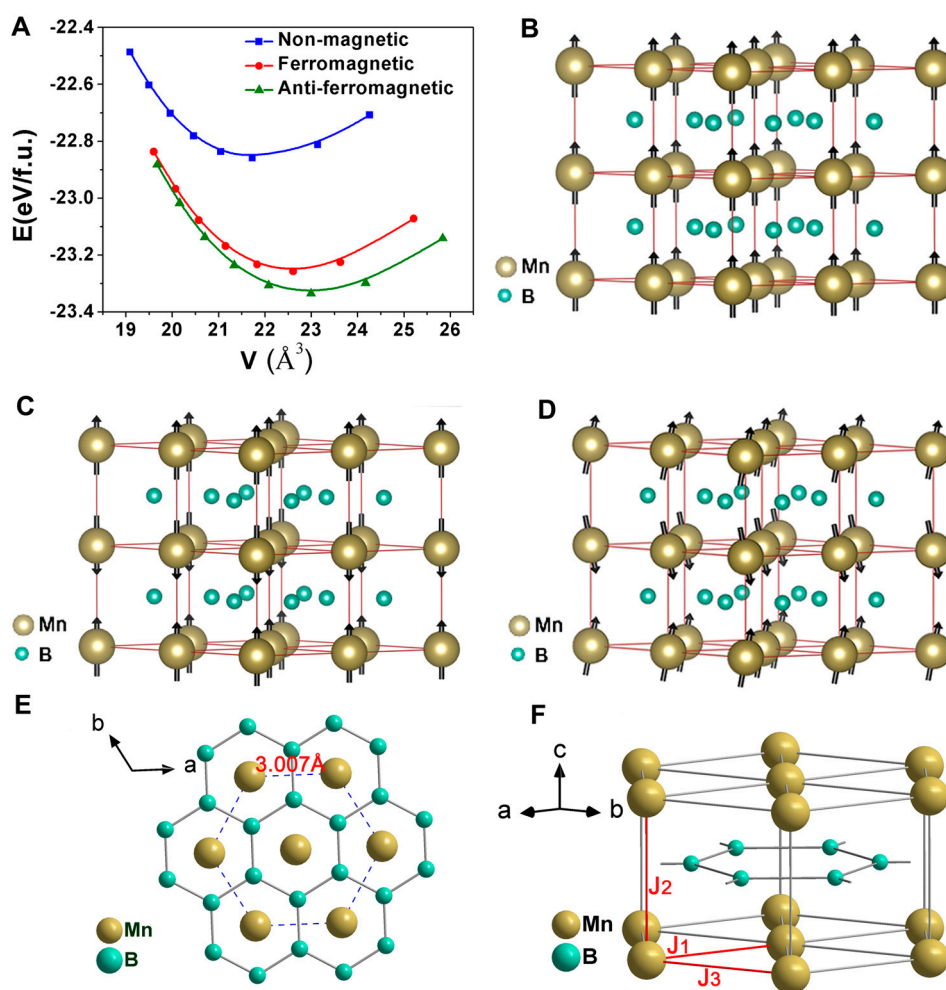
FIGURE 4
(A) Energy vs. volume (E−V) curves of different magnetic structures calculated using the PBE function. **(B−D)** Ferromagnetic, antiferromagnetic, and spin-canting antiferromagnetic structures of MnB$_2$, respectively. The large yellow spheres with arrows and the small green spheres represent the manganese and boron atoms, respectively. **(E)** The crystal structure and the atomic distance of MnB$_2$. **(F)** The crystal structure of MnB$_2$ with three NN pairs of manganese atoms.

property was found in the single MnB$_2$ crystal, signifying that ferromagnetic properties did not originate from the secondary phase [28]. Consequently, it could be concluded that the weak ferromagnetism was an intrinsic property of the synthesized polycrystalline MnB$_2$ specimen. The measured spontaneous magnetization was 11.7 emu/g, and the magnetic moments was 0.16 μ_B/Mn which were close with the previous results of 14.36 and 14.0 emu/g obtained by Kasaya and Hihara [28].

Furthermore, first-principle calculations were used to settle the dispute about the magnetic configuration of MnB$_2$. Although neutron diffraction failed to clarify the magnetic configurations, it proposed that the magnetic moment was perpendicular to c-planes [15]. Therefore, the possible magnetic configurations of MnB$_2$ may be ferromagnetic or antiferromagnetic because all magnetic moments were perpendicular to the c-planes. Moreover, the energies of ferromagnetic ordering, antiferromagnetic ordering, and non-magnetic MnB$_2$ were compared. As seen in Figure 4A, the antiferromagnetic configuration had the lowest total energy than the ferromagnetic and non-magnetic configurations,

indicating that the antiferromagnetic configuration was the ground magnetic configuration. Figures 4B–D shows ferromagnetic, antiferromagnetic, and spin-canting antiferromagnetic structures of MnB$_2$, respectively. However, the antiferromagnetic configuration failed to explain the weak ferromagnetic behavior under 135.6 K. The manganese atomic coordination in MnB$_2$ was similar to that of Mn (2c) in Mn$_3$B$_4$. The magnetic moment of Mn (2c) in Mn$_3$B$_4$ had a canting feature [29]. Consequently, the magnetic moment in MnB$_2$ may exhibit a spin-canting character. Additionally, the spin canting feature could account for the weak ferromagnetic behavior. The tentatively determined spin canting angle of Mn was about 6° [14]. Furthermore, the titling of the spin moment could tentatively explain the reason the ZFC curve was higher than the FC curve.

As shown in Figure 4E, the nearest distance between manganese atoms was 3.007 Å in manganese layers, and the interlayer distance between two manganese layers separated by the honeycomb boron layers was 3.037 Å. The high value of T$_N$ temperature indicated strong antiferromagnetic interactions between manganese atoms in

the (001) planes. The stability of the layered antiferromagnetic spin order could be explained using the Stoner model. According to the Stoner model, spontaneous ferromagnetic magnetization appears when the condition of $N_{TM}(E_F) \times I_{TM} > 1$ is satisfied. $N_{TM}(E_F)$ and I_{TM} represent the non-polarized partial density of states at the Fermi energy level and the exchange-correlation integral, respectively. Khmelevskyi and Mohn reported that the exchange-correlation integral between the adjacent manganese layers was 0.142 mRyd, and the previous results obtained by the authors of this study for the density of states at the Fermi level was 0.46 states/fu [16]. Their product was below the criterion of spontaneous ferromagnetic magnetization, giving rise to an antiferromagnetic configuration. Moreover, there was a slight spin canting of the magnetic moment due to the complicated magnetic interactions.

Itinerant band ferromagnetic model and covalent magnetism scenarios were proposed to explain the magnetic behavior of MnB_2. The itinerant band model usually applies for metallic material, while the covalent magnetism scenarios are suitable for semiconductor or insulators. MnB_2 is a metallic conductor with a resistivity of 4.0×10^{-6} Ωm at 300 K, and the increase in resistivity with temperature denoted its metallic behavior [25]. The metallic behavior of MnB_2 ruled out the possibility of covalent magnetism and suggested that the itinerant band ferromagnetic model may meet its real case. The crystal structure of MnB_2 with three nearest-neighboring (NN) manganese atom pairs is shown in Figure 4F. The exchange-correlation integral of J_1 was larger than J_2, possibly resulting in the ferromagnetic configuration in the c planes and the antiferromagnetic configuration along the c direction. However, strong covalent boron layers separated the antiferromagnetic order between the adjacent manganese layers.

4 Conclusion

Honeycomb boron layers were inserted into the host manganese matrix to tune its magnetic properties. MnB_2, a BIC, underwent weak ferromagnetic, antiferromagnetic, and paramagnetic behaviors with increased temperatures. The long-confused T_N tended to be 330 K. First-principle calculations combined with experimental results suggested that MnB_2 had an antiferromagnetic configuration with a slight canting magnetic moment. It exhibits metallic conductivity at room temperature, which confirms the itinerant band ferromagnetic model for MnB_2. The insertion of honeycomb boron layers into the manganese matrix changed the exchange-correlation between manganese atoms.

Data availability statement

The original contributions presented in the study are included in the article/Supplementary material, further inquiries can be directed to the corresponding authors.

Author contributions

HL: Writing–original draft, Writing–review and editing. SC: Writing–review and editing. YH: Writing–review and editing. YZ: Writing–review and editing. PZ: Data curation, Writing–review and editing. SM: Writing–original draft, Writing–review and editing.

Funding

Conflict of interest

The authors declare that the research was conducted in the absence of any commercial or financial relationships that could be construed as a potential conflict of interest.

Publisher's note

All claims expressed in this article are solely those of the authors and do not necessarily represent those of their affiliated organizations, or those of the publisher, the editors and the reviewers. Any product that may be evaluated in this article, or claim that may be made by its manufacturer, is not guaranteed or endorsed by the publisher.

References

1. Kuneš J, Lukoyanov AV, Anisimov VI, Scalettar RT, Pickett WE Collapse of magnetic moment drives the Mott transition in MnO. *Nat Mater* (2008) 7:198–202. doi:10.1038/nmat2115

2. Knappschneider A, Litterscheid C, George NC, Brgoch J, Wagner N, Beck J, et al. Peierls-distorted monoclinic MnB4 with a Mn-Mn bond. *Angew Chem Int Edition* (2014) 53:1684–8. doi:10.1002/anie.201306548

3. Ge J, Hu Y, Biasini M, Beyermann WP, Yin Y Superparamagnetic magnetite colloidal nanocrystal clusters. *Angew Chem Int Edition* (2007) 46:4342–5. doi:10.1002/anie.200700197

4. Park J, Hong Y-K, Kim H-K, Lee W, Yeo C-D, Kim S-G, et al. Electronic structures of MnB soft magnet. *AIP Adv* (2016) 6:055911. doi:10.1063/1.4943240

5. Seo WS, Jo HH, Lee K, Kim B, Oh SJ, Park JT Size-dependent magnetic properties of colloidal Mn3O4 and MnO nanoparticles. *Angew Chem Int Edition* (2004) 43:1115–7. doi:10.1002/anie.200352400

6. Seiro S, Koller E, Fasano Y, Fischer Ø Homogeneous strain-relaxation effects in La0.67Ca0.33MnO3 films grown on NdGaO₃. *Appl Phys Lett* (2007) 91:091913. doi:10.1063/1.2775033

7. Salamon MB, Herman RM Critical dynamics and spin relaxation in a Cu-Mn spin-glass. *Phys Rev Lett* (1978) 41:1506–9. doi:10.1103/physrevlett.41.1506

8. Pan Y, Zhou B. ZrB₂: adjusting the phase structure to improve the brittle fracture and electronic properties. *Ceramics Int* (2017) 43:8763–8. doi:10.1016/j.ceramint.2017.04.007

9. Pan Y, Zhu J. Enhancing the Vickers hardness of Yttrium borides through bond optimization. *Mater Today Commun* (2024) 38:108428. doi:10.1016/j.mtcomm.2024.108428

10. Emery N, Hérold C, d'Astuto M, Garcia V, Bellin C, Marêché JF, et al. Superconductivity of BulkCaC6. *Phys Rev Lett* (2005) 95:087003. doi:10.1103/physrevlett.95.087003

11. Gou H, Steinle-Neumann G, Bykova E, Nakajima Y, Miyajima N, Li Y, et al. Stability of MnB2 with AlB2-type structure revealed by first-principles calculations and experiments. *Appl Phys Lett* (2013) 102:061906. doi:10.1063/1.4792273

12. Andersson L, Dellby B, Myers HP Ferromagnetic MnB2. *Solid State Commun* (1966) 4:77–8. doi:10.1016/0038-1098(66)90275-4

13. Cadeville MC. Proprietes magnetiques des diborures de manganese et de chrome: MnB2 et CrB2. *J Phys Chem Sol* (1966) 27:667–70. doi:10.1016/0022-3697(66)90217-4

14. Khmelevskyi S, Mohn P. Magnetic ordering of MnB2 an abinitio calculation. *Solid State Commun* (2000) 113:509–12. doi:10.1016/S0038-1098(99)00521-9

15. Legrand E, Neov S. Neutron diffraction study of MnB2. *Solid State Commun* (1972) 10:883–5. doi:10.1016/0038-1098(72)90213-X

16. Khmelevskyi S, Mohn P Covalent magnetism, exchange interactions and anisotropy of the high temperature layered antiferromagnet MnB2. *J Phys Condensed Matter* (2012) 24:016001. doi:10.1088/0953-8984/24/1/016001

17. Ma S, Bao K, Tao Q, Xu C, Feng X, Zhu P, et al. Investigating robust honeycomb borophenes sandwiching manganese layers in manganese diboride. *Inorg Chem* (2016) 55:11140–6. doi:10.1021/acs.inorgchem.6b01685

18. Pan Y. W2AlC: a new layered MAX phase to adjust the balance between strength and ductility. *Mater Today Chem* (2024) 35:101915. doi:10.1016/j.mtchem.2024.101915

19. Pan Y, Yang F. The influence of pressure on the structural stability, mechanical, electronic and optical properties of TiH4 and VH4 tetrahydrides: a first-principles study. *Ceramics Int* (2024) 50:14856–64. doi:10.1016/j.ceramint.2024.01.401

20. Fan J, Bao K, Jin X, Xiangxu M, Defang D, Bingbing L, et al. How to get superhard MnB$_2$: a first-principles study. *J Mater Chem* (2012) 22:17630–5. doi:10.1039/c2jm31385e

21. Wang B, Li X, Wangxu Y, Yufei T. Phase stability and physical properties of manganese borides: a first-principles study. *The J Phys Chem C* (2011) 115:21429–35. doi:10.1021/jp2073683

22. Segall MD, Lindan PJD, Probert MJ, C J Pickard PJH, Clark SJ, Payne MC, et al. First-principles simulation: ideas, illustrations and the castep code. *J Phys Condensed Matter* (2002) 14:2717–44. doi:10.1088/0953-8984/14/11/301

23. Kresse G, Furthmuller J. Efficient interactive schemes for *ab initio* total-energy calculations using a plane-wave basis set. *Phys Rev B* (1996) 54:11169–86. doi:10.1103/PhysRevB.54.11169

24. Segall MD, Shah R, Pickard CJ, Payne MC Population analysis of plane-wave electronic structure calculations of bulk materials. *Phys Rev B* (1996) 54:16317–20. doi:10.1103/physrevb.54.16317

25. Lech AT, Turner CL, Lei J, Mohammadi R, Tolbert SH, Kaner RB Superhard rhenium/tungsten diboride solid solutions. *J Am Chem Soc* (2016) 138:14398–408. doi:10.1021/jacs.6b08616

26. Zhu H, Ni C, Zhang F, Du Y, Xiao JQ Fabrication and magnetic property of MnB alloy. *J Appl Phys* (2005) 97:10M512. doi:10.1063/1.1851953

27. Ma S, Bao K, Tao Q, Zhu P, Ma T, Liu B, et al. Manganese mono-boride, an inexpensive room temperature ferromagnetic hard material. *Scientific Rep* (2017) 7:43759. doi:10.1038/srep43759

28. Kasaya M, Hihara T Magnetic structure of MnB2. *J pysical Soc Jpn* (1970) 29:336–42. doi:10.1143/jpsj.29.336

29. Kasaya M, Hihara T, Kor Y Magnetic susceptibility of single crystal Mn3B4. *J.Phys So Jpn* (1971) 30:286. doi:10.1143/jpsj.30.286